Neurobiology of Disease 159 (2021) 105505

Contents lists available at ScienceDirect

Neurobiology of Disease

journal homepage: www.elsevier.com/locate/ynbdi

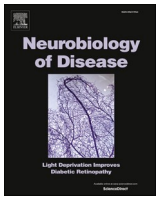

Altered cardiac structure and function is related to seizure frequency in a rat model of chronic acquired temporal lobe epilepsy

Kim L. Powell [a,b,c,1], Zining Liu [a,1], Claire L. Curl [d], Antonia J.A. Raaijmakers [d], Pragati Sharma [a,b], Emma L. Braine [a,b], Flavia M. Gomes [a], Shobi Sivathamboo [a,b,c,e], Vaughan G. Macefield [a,f], Pablo M. Casillas-Espinosa [a,b,c], Nigel C. Jones [a,b,c], Lea M. Delbridge [d], Terence J. O'Brien [a,b,c,d,*]

[a] Department of Neuroscience, Central Clinical School, Monash University, Melbourne, Australia
[b] The Department of Neurology, Alfred Health, Melbourne, Australia
[c] Department of Medicine, The Royal Melbourne Hospital, The University of Melbourne, Australia
[d] Department of Physiology, University of Melbourne, Melbourne, Australia
[e] Department of Neurology, The Royal Melbourne Hospital, Melbourne, Australia
[f] Human Autonomic Neurophysiology, Baker Heart and Diabetes Institute, Melbourne, Victoria, Australia

ARTICLE INFO

Keywords:
Temporal lobe epilepsy
Sudden unexpected death in epilepsy
Cardiac dysfunction
Cardiac fibrosis
Echocardiography

ABSTRACT

Objective: This study aimed to prospectively examine cardiac structure and function in the kainic acid-induced post-status epilepticus (post-KA SE) model of chronic acquired temporal lobe epilepsy (TLE), specifically to examine for changes between the pre-epileptic, early epileptogenesis and the chronic epilepsy stages. We also aimed to examine whether any changes related to the seizure frequency in individual animals.

Methods: Four hours of SE was induced in 9 male Wistar rats at 10 weeks of age, with 8 saline treated matched control rats. Echocardiography was performed prior to the induction of SE, two- and 10-weeks post-SE. Two weeks of continuous video-EEG and simultaneous ECG recordings were acquired for two weeks from 11 weeks post-KA SE. The video-EEG recordings were analyzed blindly to quantify the number and severity of spontaneous seizures, and the ECG recordings analyzed for measures of heart rate variability (HRV). PicroSirius red histology was performed to assess cardiac fibrosis, and intracellular Ca^{2+} levels and cell contractility were measured by microfluorimetry.

Results: All 9 post-KA SE rats were demonstrated to have spontaneous recurrent seizures on the two-week video-EEG recording acquired from 11 weeks SE (seizure frequency ranging from 0.3 to 10.6 seizures/day with the seizure durations from 11 to 62 s), and none of the 8 control rats. Left ventricular wall thickness was thinner, left ventricular internal dimension was shorter, and ejection fraction was significantly decreased in chronically epileptic rats, and was negatively correlated to seizure frequency in individual rats. Diastolic dysfunction was evident in chronically epileptic rats by a decrease in mitral valve deceleration time and an increase in E/E` ratio. Measures of HRV were reduced in the chronically epileptic rats, indicating abnormalities of cardiac autonomic function. Cardiac fibrosis was significantly increased in epileptic rats, positively correlated to seizure frequency, and negatively correlated to ejection fraction. The cardiac fibrosis was not a consequence of direct effect of KA toxicity, as it was not seen in the 6/10 rats from separate cohort that received similar doses of KA but did not go into SE. Cardiomyocyte length, width, volume, and rate of cell lengthening and shortening were significantly reduced in epileptic rats.

Significance: The results from this study demonstrate that chronic epilepsy in the post-KA SE rat model of TLE is associated with a progressive deterioration in cardiac structure and function, with a restrictive cardiomyopathy associated with myocardial fibrosis. Positive correlations between seizure frequency and the severity of the cardiac changes were identified. These results provide new insights into the pathophysiology of cardiac disease in

* Corresponding author at: Department of Neuroscience, Central Clinical School, Monash University, Melbourne, Australia.
E-mail address: Terence.OBrien@monash.edu (T.J. O'Brien).
[1] These authors contributed equally to this work.

https://doi.org/10.1016/j.nbd.2021.105505
Received 15 November 2020; Received in revised form 2 September 2021; Accepted 5 September 2021
Available online 11 September 2021

chronic epilepsy, and may have relevance for the heterogeneous mechanisms that place these people at risk of sudden unexplained death.

1. Introduction

Cardiac electrophysiological dysfunction is common in people with epilepsy; particularly in those with a longer-standing drug-resistant epilepsy (Surges et al., 2010; Fialho et al., 2018a; Chyou et al., 2016). As a result, people with epilepsy can suffer from cardiac arrhythmias such as bradyarrhythmia, resulting in episodes of syncope and tachyarrhythmias, that could be critical factors contributing to the increased risk of sudden death in people with epilepsy (Fialho et al., 2018a; Chyou et al., 2016; Shorvon and Tomson, 2011). Such deaths are termed Sudden Unexpected Death in EPilepsy (SUDEP) and are a major concern for people with epilepsy. SUDEP is the major cause of mortality in people with epilepsy, accounting for up to 38% of all deaths (Shorvon and Tomson, 2011; Ficker, 2000). High seizure frequency and poorly controlled seizures are the biggest risk factors for SUDEP (Jehi and Najm, 2008), and to further impound this burden is the fact that current anti-seizure medications are ineffective at controlling seizures in more than 30% of people with epilepsy (Kwan et al., 2011).

Despite the extensive literature on SUDEP, there has been relatively limited data on cardiac structural and functional pathology in patients with chronic epilepsy or SUDEP cases. A review by Nascimento and colleagues in 2017 revealed 11 studies covering 288 SUDEP cases that reported cardiac pathology, with cardiac abnormalities were reported in 25% of cases, with the most common findings being cardiomyocyte hypertrophy and myocardial fibrosis (Nascimento et al., 2017). Other common cardiac pathologies reported in people with epilepsy include higher mean left atrial diameter (Ramadan et al., 2013), higher LV stiffness, increased LV filling pressure and greater left atrial volume (Fialho et al., 2018b). In newly diagnosed and untreated patients with Idiopathic Generalized Epilepsy reduced ejection fraction and increased LV filling pressure have been reported (Bilgi et al., 2013).

Although animal studies could allow for deeper dissections of the mechanistic relationship of seizures and epilepsy with cardiac pathology, there are a limited number of studies in chronic epilepsy models reporting cardiac pathology, and some of these studies have reported conflicting data. In a rat model of chronic acquired epilepsy, eccentric cardiac hypertrophy was reported without significant cardiac fibrosis 2–3 months and 7–11 months after systemic kainic acid (KA) induced status epilepticus (SE) (Naggar et al., 2014). However, the animals in this study only experienced SE for 1 h, compared with 4 h which is usual for this model, and the resulting chronic spontaneous seizure frequency was highly variable, ranging from one seizure in three months to 8 seizures per week. In another study where the KA was injected directly into the hippocampus to induce SE, cardiac fibrosis was evident within 48 h of seizure induction and remained present for at least 28 days (Read et al., 2015). Functionally, left ventricular internal dimension (LVID), measured at end-diastole, was increased and left-ventricular posterior wall thickness (LVPW) was reduced, leading to decreased ejection fraction. Cardiac fibrosis has also been reported in chronically epileptic rats 75 days after pilocarpine-induced SE, although seizure frequency was not reported (Sharma et al., 2019). With different ways of inducing acquired epilepsy and different time-points studied, interpretation of these findings is difficult. Therefore, we set out to examine cardiac structure and function at three time-points in the post-status epilepticus (post-SE) rat model of epilepsy; prior to the induction of SE (pre-SE), 2 weeks (as spontaneous seizures are beginning) and 10 weeks post-SE (chronic epileptic time point). The aims of the study were to determine whether progressive structural and functional cardiac pathology developed progressively during the development of chronic epilepsy, and to assess if their severity was correlated with the severity of the epilepsy in the chronic epilepsy stage as measured by seizure frequency on continuous video-EEG monitoring.

2. Materials and methods

The experimental procedures used in this study were approved by the Florey (University of Melbourne) Animal Ethics committee (14–072), or the Alfred Medical Research & Education Precinct Animal Ethics Committee (E/1853/2018/M), with adherence to the Australia Code of Practice for the care and use of animals for scientific purposes. All animal procedures were performed under anesthesia and all efforts were made to minimize pain and discomfort to the animals. Rats were housed within the Biological Research Facility at the Royal Melbourne Hospital (University of Melbourne) or The Department of Neuroscience laboratories, Monash University, Alfred Hospital, with a constant temperature of 22 °C, 12 h light and dark cycle with ad libitum access to food and water.

2.1. Post-SE model of acquired epilepsy

The post-SE model of chronic temporal lobe epilepsy (TLE) was generated by inducing a period of continuous seizure activity (SE) in rats by administering the glutamatergic agonist, KA intraperitoneally (i.p.). This model reflects many features of TLE in humans, including histopathologic changes in limbic structures, a “latent period” following the initiating insult, and the eventual occurrence of spontaneous seizures (Casillas-Espinosa et al., 2019). Adult 10-week-old outbred male Wistar rats ($n = 9$) received repeated injections of KA (initial dose 7.5 mg/kg, subsequent dose 2.5 mg/kg every hour) until SE was induced or a maximum dose of 22.5 mg/kg had been administered (Bhandare et al., 2017). This method induces a predominantly non-convulsive SE, and has a lower mortality (approximately 25%) than the traditional single large KA injection method which produces predominantly convulsive SE and a mortality of up to 80%, while still producing a long term chronic epileptic state and histological changes of mesial temporal sclerosis (Casillas-Espinosa et al., 2019; Bhandare et al., 2017; Powell et al., 2008; Jupp et al., 2012). The control group ($n = 8$) were handled the same way with an equivalent volume of saline. Repetitious class IV (forelimb clonus with rearing) and class V motor seizures (class IV seizure characteristics with additional loss of postural control) were used to determine the onset of SE (Hellier et al., 1998). After 4 h of SE, seizures were terminated with Diazepam (i.p. 5 mg/kg). Monitoring of rats weight loss was performed for 7 days post-SE, with mush (crushed rat pellets) provided to supplement diet daily until the rats restored original weight pre-SE. Only animals that showed a stable SE for 4 h and recovered after SE termination were included in this study.

2.2. Echocardiography

Time points for echocardiography were 24 h prior to induction of SE, 2 weeks, and 10 weeks post-SE. These time points were chosen to represent the baseline period, the early epileptogenesis period before the onset of spontaneous recurrent seizures (2 weeks post-SE) and the chronic epileptic state (10 weeks post-SE) (Casillas-Espinosa et al., 2019). In our experience, animals begin to develop spontaneous seizures around 2 weeks after KA-induced SE and by 10 weeks animals are chronically epileptic (Casillas-Espinosa et al., 2019; Powell et al., 2008; Powell et al., 2014). Cardiac structure and function were evaluated by transthoracic 2-dimensional B- and M-mode echocardiography performed under light anesthesia (inhalation of isoflurane at 1.5%). Acquisition and offline analysis were performed with EchoPac software (GE Healthcare). The parasternal short axis was utilized for systolic

parameters namely, interventricular septum (IVS), LVPW, LVID, fractional shortening (FS), ejection fraction (EF), heart rate (HR). Mitral valve blood flow and tissue Doppler were measured in apical four chamber view for diastolic parameters (E & A wave velocity, E/A, mitral valve deceleration time MVDecT, E' velocity, E'/E). Left ventricular weights were calculated and indexed to body weight from the formula LV mass = $1.04\times[(\text{LVIDd}+\text{IVSd}+\text{LVPWd})^3-(\text{LVIDd})$ (Chyou et al., 2016)]/body weight. Relative wall thickness (RWT) was calculated by using the formula RWT = (2xLVPWd) / LVIDd. For each measurement at least three consecutive cycles were sampled.

2.3. Electroencephalogram (EEG) and Electrocardiography (ECG) electrode implantation

Surgery to implant two ECG and four EEG electrodes (PlasticOne®, USA) was performed either 2 weeks prior to, or 10 weeks post-SE after the final echocardiogram under isoflurane anesthesia (5% during induction, 2.5–1.5% for maintenance) in oxygen (2.0 L/min during induction, 0.5–1.0 L/min for maintenance) in post-SE rats and saline treated controls as previously described (Powell et al., 2014). Four holes were drilled through the cranium to position EEG electrodes above the dura: two recording electrodes on left frontal bone and left parietal bone, two referencing electrodes on right parietal bone and right parietal bone. Two ECG electrodes were implanted subcutaneously above the base of the heart and the apex of the heart with cables threaded through from thoracic location towards the cranium. Six electrodes were then plugged into a multichannel pedestal fixed onto the skill using acrylic dental cement.

2.4. EEG-ECG recordings and analysis

One week after recovery from surgery (i.e. 11 weeks post-KA SE) a two-week continuous video-EEG-ECG recording was acquired using Profusion 3 EEG acquisition software (Compumedics, Australia) at a sampling rate of 512 Hz. The rats were connected to and EEG amplifier with both EEG and ECG signals being recorded. EEG recordings from both post-SE rats and control rats were analyzed manually in a blinded manner using Profusion EEG4 v4.3 with seizure activity being defined as a paroxysmal electro-clinical event, with oscillating EEG activity that evolved in frequency and amplitude and had a duration of greater than 10 s, as per previous studies from our laboratory (Casillas-Espinosa et al., 2019; Powell et al., 2008; Powell et al., 2014). Video recordings were utilized to visually verify the accompanying behavioural manifestations of the seizure. Start and finish times of seizures were recorded to allow for the quantification of the duration of seizures. For heart rate changes during spontaneous seizures, four to five seizures were randomly selected from four animals and heart rate (BMP) was calculated for the entire period of the seizure including 20 s prior to seizure onset and up to 100 s after seizure end. Seizures occurring before EEG/ECG recording were not evaluated.

2.5. Heart rate variability analysis (HRV)

Five-minute interictal segments of sleep (between 7 and 9 am) and wakefulness (between 7 and 9 pm) ECG were selected from each animal at rest during the two week continuous video-EEG recording period from weeks 11–13 post-KA SE. Segments were imported into LabChart Pro 8·1·13 (ADinstruments, Dunedin, New Zealand) for HRV analysis and the time of each R-wave was marked. We reported time domain and spectral components of HRV using recommended international HRV guidelines (Malik, 1996). Time-domain HRV parameters generated included the standard deviation of the normal-to-normal (NN) intervals (SDNN) and root mean square of the successive differences (RMSSD). Spectral components included low-frequency power (LFP) between 0·04–0·15 Hz and high-frequency power (HFP) between 0·15–0·4 Hz. We reported individual spectral components as normalized units.

2.6. Cardiac tissue collection

After completion of the two-week EEG recordings rats were anesthetized with 5% isoflurane and oxygen (2.0 L/min) followed by Lethabarb (1 mL, Virbac) intraperitoneally prior to decapitation. Hearts were rapidly removed and washed rapidly in Deca Krebs (NaCl 146 mM, KCl 4.7 mM, NaH_2PO_4 0.35 mM, $MgSO_4{\bullet}7H_2O$ 1 mM, $C_6H_{12}O_6$ 11 mM) with HEPES buffer (10 mM) and 4 μM $CaCl_2$ with pH 7.4 and then in Deca Krebs with HEPES buffer, as above minus the 4 μM $CaCl_2$. Hearts were then trimmed of excess connective and adipose tissue before being blotted dry and weighed. Hearts were then cut transversely at the level of the papillary muscle and fixed in 4% neutral buffer formaldehyde for histologic analysis.

2.7. Histological analysis

After fixation, hearts were sent for histological preparation (Biomedical Sciences Histology Facility, The University of Melbourne, Australia). Tissue sections were embedded in paraffin, sectioned at 5 μm and stained for PicroSirius red histochemistry. *Fibrosis Quantification:* PicroSirius red stained sections were imaged at 20× and using Stereoinvestigator, images were collated to provide a complete transverse image of the heart. Using an Olympus BX51 microscope and Stereo Investigator, QI camera, PicroSirius red stained sections were imaged at 20× magnification followed by collation of images to form a complete transverse image of the heart. Images were processed using an automated image analyzer (ImageJ version 1.52a) to quantify fibrosis. Threshold colors were adjusted using the Hue-Saturation-Brightness combination to identify red highlighted pixels representing fibrosis area and whole heart area. Total fibrosis and whole heart areas measured in pixels were corrected by excluding red stained areas representing perivascular regions and staining artefacts (manually demarcated by user) (See Supporting Fig. 1). The percentage of fibrosis was quantified by calculating ratio of total fibrosis area to total whole heart area (x 100) for each image analyzed.

2.8. Cardiomyocyte isolation

Rat left ventricular cardiomyocytes were isolated enzymatically using methods previously described (Curl et al., 2018).

2.9. Cardiomyocyte intracellular Ca^{2+} and contractility measurements

Intracellular Ca^{2+} and cell length were measured simultaneously by microfluorimetry and edge detection (Ionoptix MA, USA) as previously described (Curl et al., 2018). Animal numbers varied for these measurements due to cardiac tissue availability after tissue collection for histology and molecular biology (not presented in this paper).

2.10. Kainic acid-resistant cohort

To address the question of whether the use of systemic kainic acid injection to induce status epilepticus could have a direct toxic effect on the heart that could confound the assessment of the relationship between the cardiac changes and the chronic epilepsy, we studied an additional cohort of 10 week old male Wistar rats who received KA but were resistant to entering SE, and did not develop chronic spontaneous seizures. On occasions in our research program we encounter cohorts of rats in whom a proportion show resistance to KA induced SE. In this cohort, there were 6 out of 10 rats who received the maximal allowed dose of KA (total dose 22.5 mg/kg) but did not enter SE (as verified by EEG and behavior). None of these 6 animals exhibited spontaneous seizures in the chronic period (as verified from blinded assessment of EEG recordings conducted 12 weeks post-SE). In contrast all 4 of the rats in this cohort that did go into SE with the KA injections manifested spontaneous seizures on the video-EEG recordings at 12 weeks. At the

conclusion of the EEG monitoring period, 13 weeks post-SE, these animals were sacrificed, their hearts extracted and processes for histological analysis, as described above. A comparison of fibrosis level on histological examination of the hearts rats was made between the KA-resistant rats ($n = 6$), the post KA SE rats ($n = 4$) and 4 vehicle treated control rats who underwent identical procedures.

2.11. Statistical analysis

The primary outcomes assessed were seizure frequency, heart rate, heart rate variability (HRV), cardiac morphological, systolic and diastolic changes, amount of cardiac fibrosis and cardiomyocyte contractility. All data was analyzed using GraphPad Prism v.5. Echocardiography data was analyzed using 2-way analysis of variance (ANOVA) for repeated measures with treatment (saline and post-SE) and time as the 2 independent variables. Treatment x time pairwise comparisons (each of the three time points comparing saline controls to post-SE rats) were assessed using Bonferroni post hoc analysis. Calcium contractility, histological and HRV data were analyzed by comparing saline controls to post-SE rats using two-tailed Mann-Whitney *U* test. A variable in which seizure frequency was compared to ejection fraction or cardiac fibrosis, an XY analysis – nonlinear regression with the log of both x and y variables with r-squared was performed. Data were expressed as means with standard deviations (mean ± SD) or medians with interquartile ranges (IQR). The spearman rank correlation coefficients were used to examine the correlation between HRV measures and seizure frequency in the post-SE group. Statistical significance was set at $p < 0.05$. All statistical tests were performed using GraphPad Prism version 5 (La Jolla, California, United States).

3. Results

3.1. Chronically epileptic rats show dramatic changes in heart during spontaneous seizures

Twelve 10-week-old male Wistar rats were injected with KA (total doses up to total dose 22.5 mg/kg), with 9 rats going into SE lasting which was terminated with diazepam after 4 h and then recovering, while 3 rats died during or immediately following the SE. All surviving post-SE rats ($n = 9$) had spontaneous seizures recorded on the two-week continuous video-EEG monitoring commencing 11 weeks following the KA-induced SE, whereas the saline control rats ($n = 8$) had no spontaneous seizures. The mean ± standard error animal weight at 11 weeks post-SE in epilepsy group and control group are 480.4 ± 28.6 g and 583.4 ± 42.2 g, respectively. As shown in Fig. 1A seizure frequency varied from 0.3 to 10.6 seizures/day and seizure duration ranged from 11 to 62 s with a mean of 38 s. An example of an ECG trace during a spontaneous seizure is shown in Fig. 1B with periods of tachycardia (increased heart rate) and bradycardia (reduced heart rate) clearly shown. Chronically epileptic rats show dramatic changes in heart rate during spontaneous seizures. Fig. 1C-F shows heart rate changes during 4–5 spontaneous seizures in 4 different chronically epileptic post-SE rats. In the majority of cases bradycardia occurs at, or just prior to, seizure onset, with heart rate dropping to around 100 bpm in some severe cases. Furthermore, in some cases heart rate had not returned to baseline for up to 2 min after the seizure had ended (Fig. 1C-F).

3.2. Morphological changes in the heart during epileptogenesis

Fig. 2A and B show an example of echocardiographic 2D M-mode parasternal short axis images from a saline (Fig. 2A) and chronically epileptic post-SE rat (Fig. 2B) highlighting changes in left ventricular diameter during the cardiac cycle. 2-factorial analysis revealed significant main effects of treatment (saline and post-SE) ($F_{1,44} = 4.18$, $P = 0.04$, ANOVA) but no effect of time ($F_{2,44} = 0.13$, $P = 0.88$, ANOVA) on left ventricular posterior wall thickness (LVPWd). Each time point comparison showed no difference between saline control and post-SE rats prior to, and 2 weeks post-SE, however chronically epileptic rats 10 weeks post-SE ($M = 1.92$, $SD = 0.27$) showed significantly thinner posterior wall thickness compared to 10 week saline controls ($M = 1.59$, $SD = 0.21$; t[9,7] = 2.55, $P = 0.04$, Bonferroni; Fig. 2C). A significant effect of treatment ($F_{1,44} = 9.54$, $P = 0.004$, ANOVA) and time ($F_{2,44} = 11.64$, $P \leq 0.001$, ANOVA) was observed on the left ventricular internal dimension (LVIDd), or left ventricular chamber diameter. LVIDd was not significantly different between saline control and post-SE rats prior to and at 2 weeks post-SE, however 10 weeks post-SE rats ($M = 8.26$, $SD = 0.37$) showed smaller chamber diameters compared to their respective saline controls ($M = 9.05$, $SD = 0.19$; t[9,7] = 3.04, $P = 0.01$, Bonferroni; Fig. 2D). Relative wall thickness (RWT), a ratio of the LVPWd and LVIDd was not significantly different between saline controls and post-SE rats at all 3 epileptogenic time-points (Fig. 2E), indicating the absence of both hypertrophy and dilation in these hearts. For LV mass, a significant interaction ($F_{2,44} = 6.20$, $P = 0.004$, ANOVA) between treatment and time was found with effects of both treatment ($F_{1,44} = 10.01$, $P = 0.003$, ANOVA) and time ($F_{2,44} = 4.62$, $P = 0.015$, ANOVA). LV mass was significantly reduced in chronically epileptic rats 10 weeks post-SE ($M = 0.73$, $SD = 0.12$) compared to saline controls ($M = 0.99$, $SD = 0.11$) at the same time-point (t[9,7] = 4.40, $P < 0.001$, Bonferroni; Fig. 2F) indicating that hearts from post-SE rats were reduced in size relative to control. All morphology measured by echocardiography is shown in Table 1.

3.3. Chronically epileptic post-SE rats show systolic dysfunction

Systolic dysfunction was evident as reduced ejection fraction in chronically epileptic rats ($M = 65.55$, $SD = 5.68$) compared to saline controls ($M = 80.36$, SD 3.60) 10 weeks post-SE (t[9,7] = 5.37, $P < 0.001$, Bonferroni) but not at 2 weeks post-SE (Fig. 2G). In addition, a significant interaction ($F_{2,44} = 8.14$, $P = 0.001$, ANOVA) was observed between treatment and time with main effects of both treatment ($F_{1,44} = 15.04$, $P < 0.001$, ANOVA) and time ($F_{2,44} = 7.06$, $P = 0.002$, ANOVA) on ejection fraction. There was a 15% reduction (saline controls 80% compared to post-SE 65%) in the amount of blood ejected from the LV with each contraction in chronically epileptic rats 10 weeks post-SE compared to saline controls at the same time point. Importantly, ejection fraction had a negative correlation with the number of seizures/day (Fig. 2H) whereby post-SE rats with higher number of seizures had the lowest ejection fraction. The most chronically epileptic post-SE rat that had 10.6 seizures/day had the lowest ejection fraction of 57.5%. Cardiac output was also significantly reduced in the chronically epileptic rats 10 weeks post-SE compared to controls (Table 1). All systolic parameters measured by echocardiography is shown in Table 1.

3.4. Diastolic dysfunction in chronically epileptic post-SE rats is evident before systolic dysfunction

Representative blood flow Doppler and tissue Doppler images from a saline control and a chronically epileptic 10-week post-SE rat are shown in Fig. 3A-D. The early phase (E) of ventricular filling during diastole occurs when the mitral valve opens, and blood passively moves into the LV. This is followed by the late phase (A) of LV filling resulting in the last of blood in the LA being pushed into the LV due to atrial contraction. In a healthy heart the E (or E`) velocity should be greater than the A (or A`) velocity (Fig. 3A & C) but as evident in Fig. 3D the E` velocity in chronically epileptic rats 10 weeks post-SE is reduced compared to the A` velocity indicative of reduced movement of the ventricle wall surrounding the mitral valve. Early filling of the LV showed no significant difference in the velocity of blood flow through the mitral valve between saline control and chronically epileptic rats 10 weeks post-SE (Table 2). However, the mitral valve deceleration time (the time taken for the passive flow of blood into the ventricle from the atria) was significantly reduced 2 ($M = 42.30$, $SD = 7.74$; t[8,7] = 2.56, $P = 0.04$, Bonferroni)

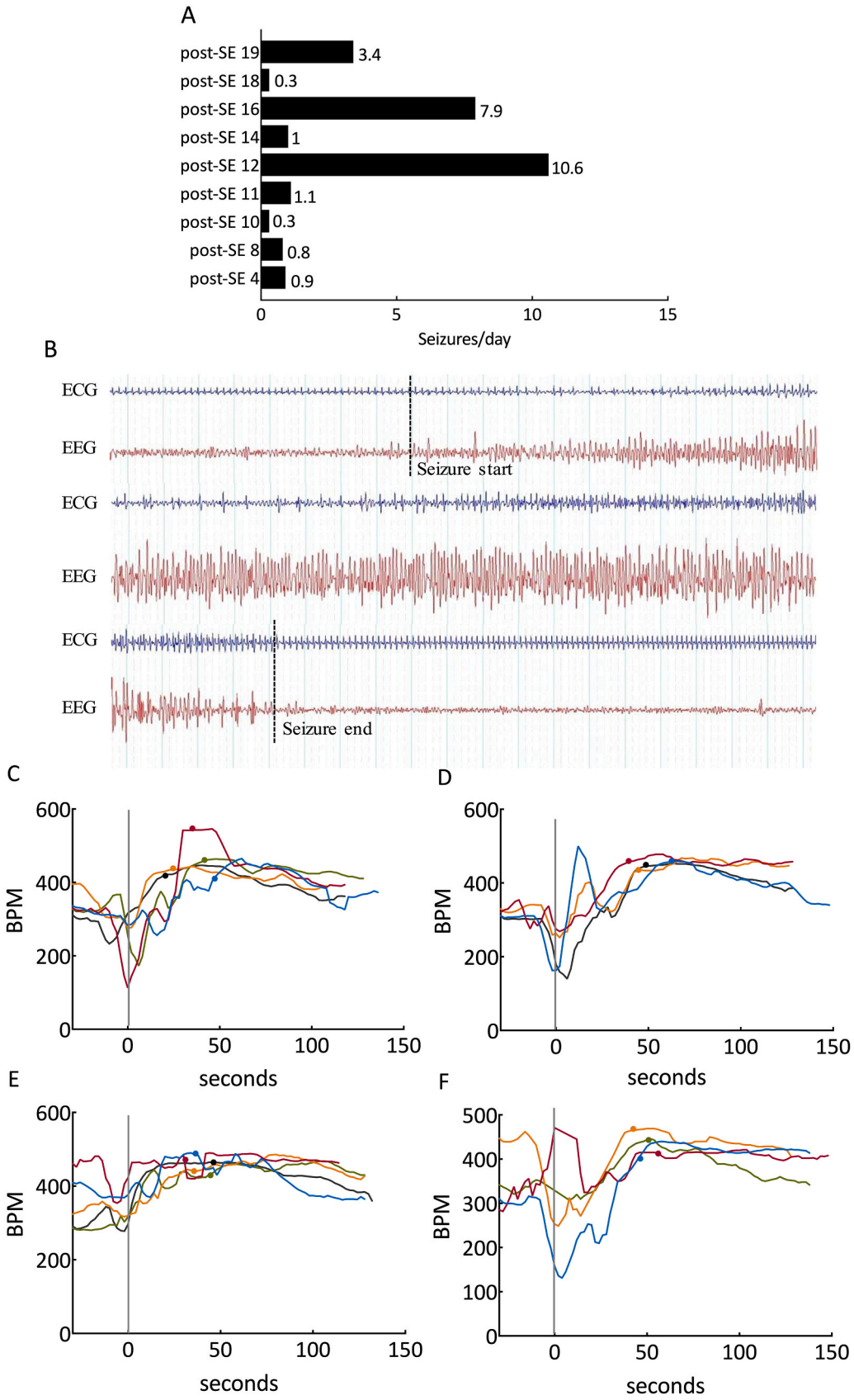

Fig. 1. Seizure data and changes in heart rate during spontaneous seizures in chronically epileptic post-SE rats recorded on continuous video-EEG monitoring from 11 to 13 weeks post-KA SE. (A) Average seizure frequency per day over the two-week continuous video-EEG recording for each post-SE rat. (B) Example EEG and ECG trace during a typical spontaneous seizure in a post-SE rat showing changes in heart rate during a seizure. (C—F) Changes in heart rate during 4–5 example spontaneous seizures in 4 different chronically epileptic post-SE rats (the dot on each trace signifies the timing of the seizure end on the EEG).

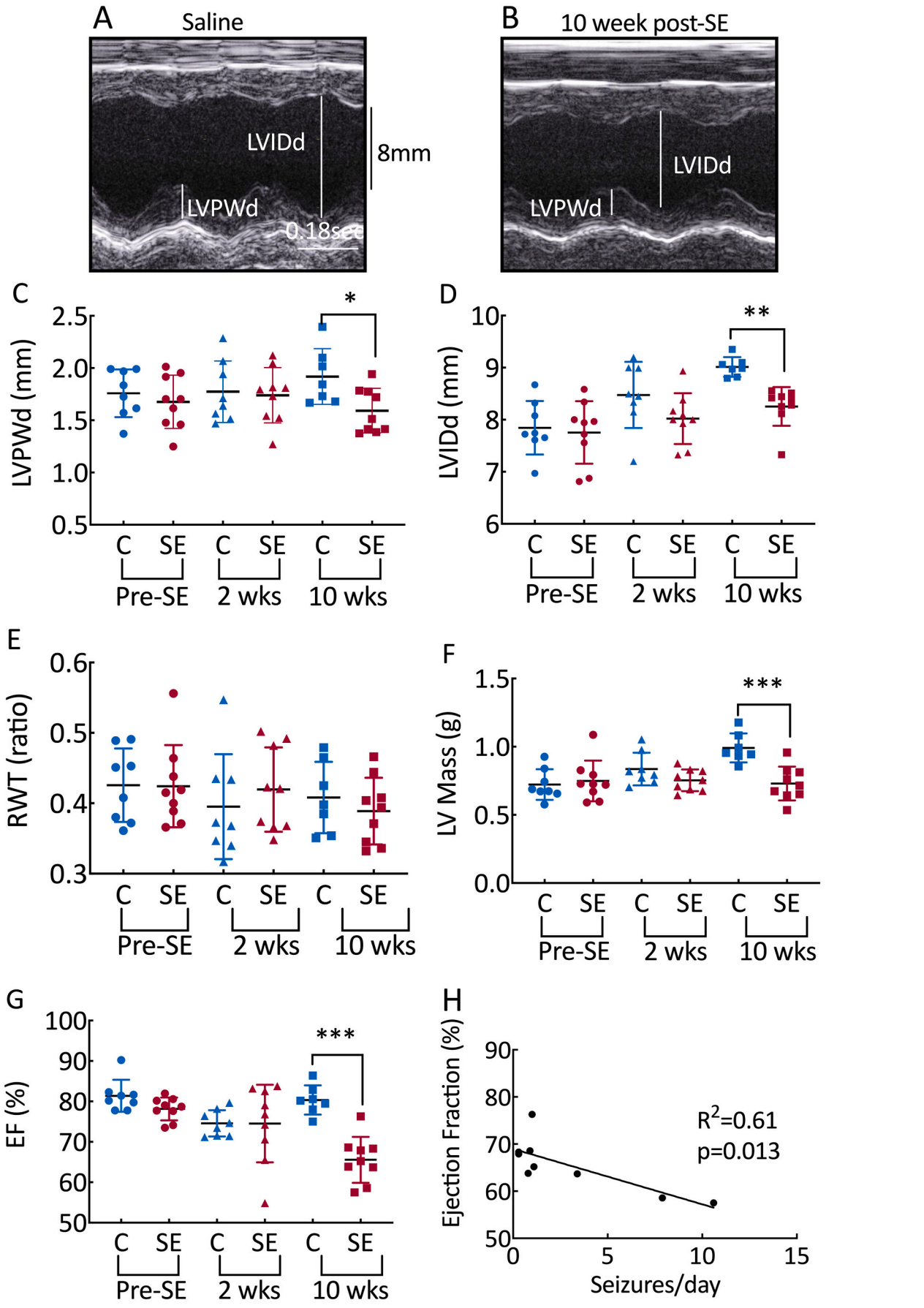

(caption on next page)

Fig. 2. Morphological and systolic functional changes during epileptogenesis. Echocardiographic 2D M-mode parasternal short axis images from a saline (A) and post-SE (B) rat showing changes in left ventricular diameter during the cardiac cycle. (C) Left ventricular posterior wall thickness (LVPWd) and (D) left ventricular internal dimension (LVIDd) at diastole was significantly reduced 10 weeks post-SE compared to saline controls. (E) There was no significant difference in relative wall thickness at any time-point whereas LV mass (F) was significantly decreased 10 weeks post-SE compared to saline controls. Reduced ejection fraction (G) was observed 10 weeks post-SE with the number of seizures/day being negatively correlated to ejection fraction (H). C = control; SE = post-SE. 2-way repeated measures ANOVA with Bonferroni post-hoc test *$p < 0.05$, **$p < 0.01$, ***$p < 0.001$; control $n = 8$, post-SE $n = 9$.

Table 1
Morphological, systolic and diastolic echocardiographic data pre-SE, 2- and 10-weeks post-SE.

		Pre SE		2 weeks post-SE		10 weeks post-SE	
Systolic Parameter		Control	SE	Control	SE	Control	SE
IVSd	mm	1.57 ± 0.05	1.58 ± 0.05	1.54 ± 0.04	1.59 ± 0.05	1.75 ± 0.07	1.59 ± 0.05
IVSs	mm	2.54 ± 0.09	2.46 ± 0.06	2.55 ± 0.09	2.50 ± 0.8	2.89 ± 0.09	2.43 ± 0.06
LVPWd	mm	1.76 ± 0.08	1.61 ± 0.08	1.77 ± 0.010	1.76 ± 0.08	1.92 ± 0.10	1.56 ± 0.07*
LVPWs	mm	2.60 ± 0.15	2.50 ± 0.10	1.75 ± 0.08	2.59 ± 0.07	2.85 ± 0.10	2.08 ± 0.09
LVIDd	mm	7.85 ± 0.18	7.85 ± 0.16	8.48 ± 0.22	7.99 ± 0.15	9.01 ± 0.07	8.25 ± 0.11**
LVIDs	mm	4.78 ± 0.21	4.74 ± 0.014	5.16 ± 0.20	5.01 ± 0.18	5.64 ± 0.14	5.84 ± 0.14
RWT	ratio	0.43 ± 0.02	0.41 ± 0.02	0.40 ± 0.03	0.42 ± 0.02	0.41 ± 0.02	0.38 ± 0.02
LV mass	g	0.72 ± 0.04	0.75 ± 0.04	0.84 ± 0.04	0.75 ± 0.02	0.99 ± 0.04	0.72 ± 0.04***
CO	ml/s	5.04 ± 0.22	4.92 ± 0.27	6.18 ± 0.37	5.17 ± 0.26	6.74 ± 0.31	4.39 ± 0.19***
FS	%	92.22 ± 1.69	39.68 ± 1.08	39.23 ± 1.18	37.38 ± 1.39	37.41 ± 1.31	29.29 ± 1.10
EF	%	81.40 ± 1.40	79.11 ± 1.08	74.57 ± 1.15	73.896 ± 2.92	75.52 ± 1.53	61.58 ± 1.68***
HR	bpm	382.10 ± 8.67	365.98 ± 5.37	376.68 ± 9.52	381.46 ± 6.68	385.22 ± 8.46	350.11 ± 5.10
Diastolic Parameter							
E wave velocity	mm/s	640.24 ± 30.7	619.66 ± 3.1.5	666.89 ± 41.4	572.88 ± 3.62	614.99 ± 22.0	576.70 ± 14.8
A wave velocity	mm/s	528.08 ± 37.6	590.26 ± 36.5	545.72 ± 44.8	537.00 ± 48.4	528.64 ± 24.6	512.84 ± 37.5
E/A ratio	ratio	1.28 ± 0.15	1.06 ± 0.02	1.27 ± 0.08	1.14 ± 0.011	1.23 ± 0.11	1.18 ± 0.08
MV Dec T	ms	41.54 ± 2.7	56.13 ± 4.8	58.08 ± 2.4	44.58 ± 3.3*	57.85 ± 2.9	33.50 ± 3.2***
E` velocity	mm/s	78.05 ± 8.0	79.72 ± 8.9	83.43 ± 8.1	55.52 ± 6.1**	84.37 ± 9.0	43.45 ± 3.7**
E/E`	ratio	8.56 ± 0.7	8.48 ± 0.7	8.51 ± 0.8	11.84 ± 1.2*	7.87 ± 0.9	15.31 ± 1.1***

IVSd – interventricular septum at diastole; IVSs – interventricular septum at systole; LVPWd – left ventricular posterior wall at diastole; LVPWs – left ventricular posterior wall at systole; LVIDd – left ventricular inner diameter at diastole; LVIDs – left ventricular inner diameter at systole; RWT – relative wall thickness; LV Mass – left ventricular mass; CO – cardiac output; FS – fractional shortening; EF – ejection fraction; HR – heart rate; SE – status epilepticus. MV DecT – mitral valve deceleration time. (*$p < 0.05$, **$p < 0.01$, ***$p < 0.001$, Two-way repeated measures ANOVA with Bonferroni post-hoc test, n = 8–9 hearts/group).

and 10 ($M = 33.20$, $SD = 10.16$; t[10,7] = 4.20, $P < 0.001$, Bonferroni) weeks post-SE compared to saline controls (2 weeks post-SE ($M = 58.08$, $SD = 6.35$), 10 weeks post-SE ($M = 57.85$, $SD = 7.56$); Fig. 3E). This is seen as an increased downward slope of the E wave in the blood flow Doppler images (Fig. 3B) and is indicative of increased wall stiffness. For mitral valve deceleration time, the interaction ($F_{2,46} = 10.44$, $P < 0.001$, ANOVA) between treatment and time was significant with effects of treatment ($F_{1,46} = 8.89$, $P = 0.004$, ANOVA) but not of time. Furthermore, the E/E` ratio (the ratio of early blood flow to mitral wall motion which is a surrogate measure of LV filling pressure) is significantly increased 2 ($M = 12.46$, $SD = 3.48$; t[9,8] = 2.99, $P = 0.013$, Bonferroni) and 10 ($M = 15.97$, $SD = 2.97$; t[9,7] = 5.92, $P < 0.001$, Bonferroni) weeks post-SE compared to saline controls (2 weeks post-SE ($M = 8.51$, $SD = 2.13$), 10 weeks post-SE ($M = 7.87$, $SD = 2.49$); Fig. 3F) confirming diastolic dysfunction in these groups. All diastolic parameters measured by echocardiography is shown in Table 1.

3.5. Heart rate variability (HRV) on ECG

3.5.1. Time-domain components of HRV

The standard deviation of the normal-to-normal (NN) intervals (SDNN) did not differ between post-SE rats and controls in either sleep or wakefulness (Table 4). The root mean square of the successive differences (RMSSD) was significantly lower in wakefulness in the post-SE group (median 6.12, interquartile range [IQR] 3.88–10.25) compared to controls (median 10.72, (IQR 9.32–17.24; $p = 0.036$). However, no between-group differences were observed to the RMSSD in sleep.

3.5.2. Spectral components of HRV

The normalized LFP of the HRV in wakefulness significantly higher in post-SE rats than controls ($p = 0.012$). However, normalized LFP in sleep was similar among post-SE rats and controls. The normalized units of HFP were similar among post-SE rats and controls in both sleep and wakefulness.

3.5.3. Correlation between HRV and seizure frequency in post-SE rats

In a correlation analysis in post-SE rats, we found a positive correlation in sleep between seizure frequency and both the time-based measures SDNN ($p = 0.018$) and RMSSD ($p = 0.041$) during sleep (Table 5).

3.5.4. Cardiac fibrosis is positively correlated to seizure frequency

Representative PicroSirius red histochemistry images from a control rat and post-SE rats having one and 10 seizures per day is shown in Fig. 4A-C with red areas indicating increased collagen deposition. Chronically epileptic post-SE rats had significantly more cardiac fibrosis than compared to saline controls (Fig. 4D, $p < 0.001$). Furthermore, there was a significant positive correlation between the percentage of fibrosis and seizure frequency (Fig. 4E, $R^2 = 0.848$, $p = 0.0004$) and a negative correlation between the percentage of fibrosis and ejection fraction (Fig. 4F, $R^2 = 0.467$, p = 0.04), with the most chronically epileptic post-SE rat that had 10.6 seizures/day had the highest amount of fibrosis of 15.5% and the lowest ejection fraction of 57.5%.

3.5.5. Cardiac fibrosis is not directly caused by kainic acid toxicity

Representative PicroSirius Red histochemistry images from heart tissue from a post-SE rat, a KA-resistant rat and a control rat is shown in Figure 6A. The percentage of collagen area was significantly higher in the chronically epileptic post-SE group ($n = 4$) compared to the KA-resistant group ($n = 6$, $p = 0.017$, F = 7.120) and to the vehicle treated control group (n = 4, p = 0.018) (Fig. 6B).

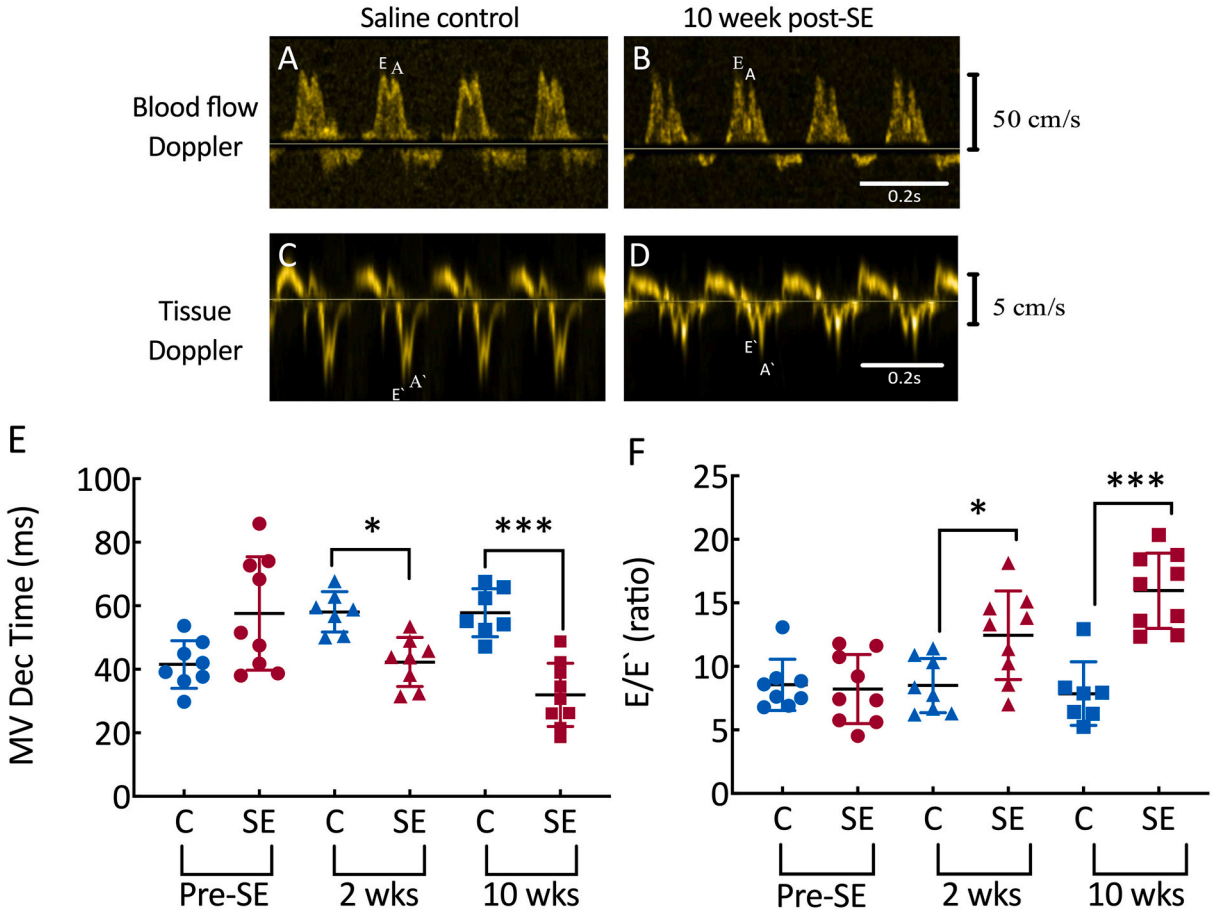

Fig. 3. Diastolic functional changes during epileptogenesis. Blood flow Doppler images from a saline control (A) and a chronically epileptic 10-week post-SE rat (B) and tissue Doppler images from a saline control (C) and chronically epileptic 10-week post-SE rat (D). The mitral valve deceleration time of the early filling phase was significantly reduced in epileptic rats 2- and 10-weeks post-SE compared to saline controls (E). The E/E` ratio (the ratio of early blood flow to mitral wall motion) is significantly increased 10 weeks post-SE compared to saline controls (F). C = control; SE = post-SE; E = Early phase of ventricular filling during diastole; A = late phase of ventricular filling during diastole. 2-way repeated measures ANOVA with Bonferroni post-hoc test *p < 0.05, ***p < 0.001; control n = 8, post-SE n = 9.

Table 2
Cardiac and cardiomyocyte morphology.

Parameter	Control	Post-SE
Heart Weight (mg)	2771.67 ± 630.01(3)	2025.00 ± 86.12 (7)
Myocyte Length (mm)	145.48 ± 10.56 (3)	133.08 ± 2.79 (7)****
Myocyte Width (mm)	34.57 ± 2.55 (3)	32.26 ± 0.87 (7)***
Myocyte Volume (pL)	40.25 ± 6.05 (3)	32.56 ± 1.48 (7)****

n hearts in parentheses, myocyte dimensions measured from mean $n = 50$ cells per heart. ***p < 0.001, ****$p < 0.0001$ Two-tailed Mann-Whitney U test; n = 3–7 hearts/group.

3.5.6. Slowed cardiomyocyte relaxation and re-uptake of Ca^{2+} into the sarcoplasmic reticulum in post SE rats

A significant reduction in cardiomyocyte length, width and volume was apparent in 10 weeks post-SE rats when compared with saline control (Table 2) determined microscopically from single myocyte dimensions. Functional analysis of shortening performance in isotonically contracting isolated intact cardiomyocytes revealed a significant reduction in percentage shortening in chronically epileptic post-SE rats when compared with saline control 10 weeks post-SE (Fig. 5A-C, Table 3). Interestingly, the post-SE cardiomyocytes displayed a significantly reduced rate of cell lengthening (MRL) indicating a slowing in relaxation of the cardiomyocytes from this group (Fig. 5D). When the MRL was plotted against seizure number no significant correlation was found indicating that changes in cardiomyocyte relaxation properties were not linked to seizure frequency (Fig. 5E).

Diastolic, systolic and amplitude Ca^{2+} were all unchanged in post-SE cardiomyocytes (Fig. 5F-H; Table 3) when compared with saline control. The rate of decay of the Ca^{2+} transient, tau, (Fig. 5I) which in the rat is a measure of Ca^{2+} reuptake into the sarcoplasmic reticulum (SR) and is an indicator of relaxation in the cardiomyocyte was slowed in the post-SE cardiomyocytes. Interestingly, a strong positive correlation between tau and seizure number was also apparent (Fig. 5J) indicating that the higher the number of seizures, the slower the rate of relaxation of the calcium transient.

4. Discussion

This study set out to longitudinally investigate the functional and structural changes that occur during epileptogenesis, and in chronic epilepsy, in the post-KA SE rat model of acquired TLE. A building body of research has highlighted many structural and functional cardiac alterations in patients (Surges et al., 2010; Fialho et al., 2018a; Chyou et al., 2016; Nascimento et al., 2017; Ramadan et al., 2013; Fialho et al., 2018b; Bilgi et al., 2013) and in animals (Naggar et al., 2014; Powell et al., 2014) with chronic epilepsy, but has not established a direct association with the epilepsy. The incidence and mechanisms of the cardiac structural abnormalities in PWE remain poorly understood. The risk of sudden death is markedly elevated in people with chronic epilepsy compared to the general community (Shorvon and Tomson, 2011; Ficker, 2000; Ficker et al., 1998; Nightscales et al., 2020). However,

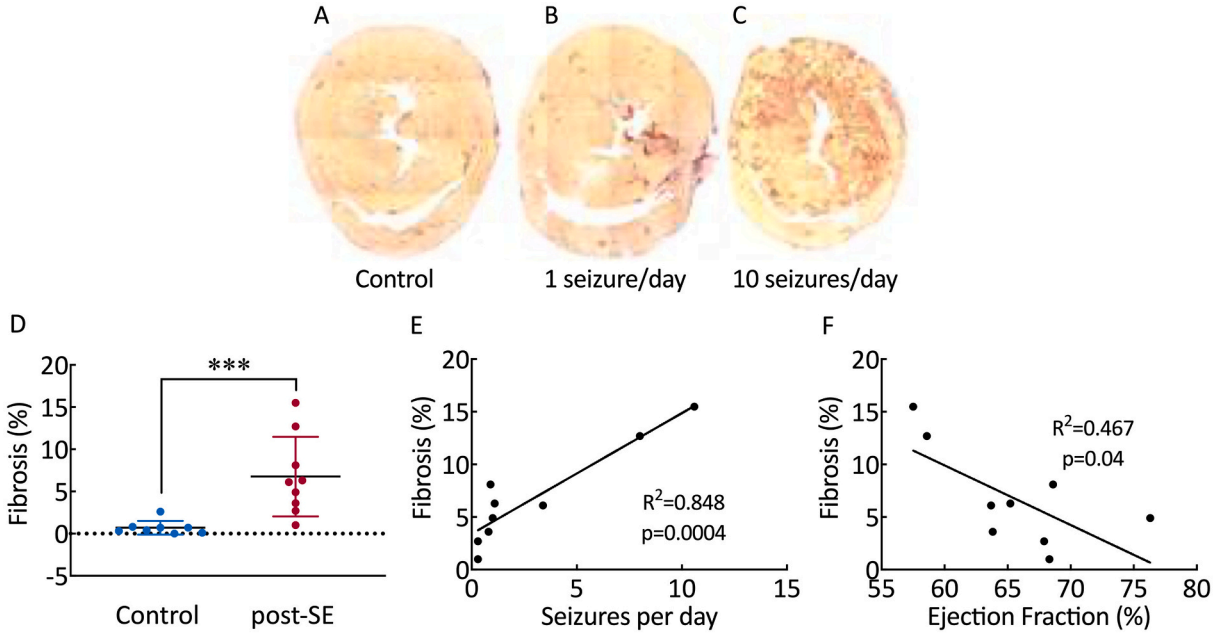

Fig. 4. Cardiac fibrosis is positively correlated to seizure frequency. (A) Transverse sections of the heart showing normal fibrosis deposition in a control rat compared to increased fibrosis deposition in post-SE rats with seizure frequency of 1 seizure/day (B) and 10 seizures/day (C) as indicated by PicroSirius red histochemistry (red areas indicate increased collagen deposition). Chronically epileptic rats 10 weeks post-SE had significantly more cardiac fibrosis compared to saline controls (D). The amount of fibrosis positively correlated with seizure frequency (E) and negatively correlated with ejection fraction (F). Two-tailed Mann Whitney *U* test ***p < 0.001; control n = 8, post-SE n = 9. (For interpretation of the references to colour in this figure legend, the reader is referred to the web version of this article.)

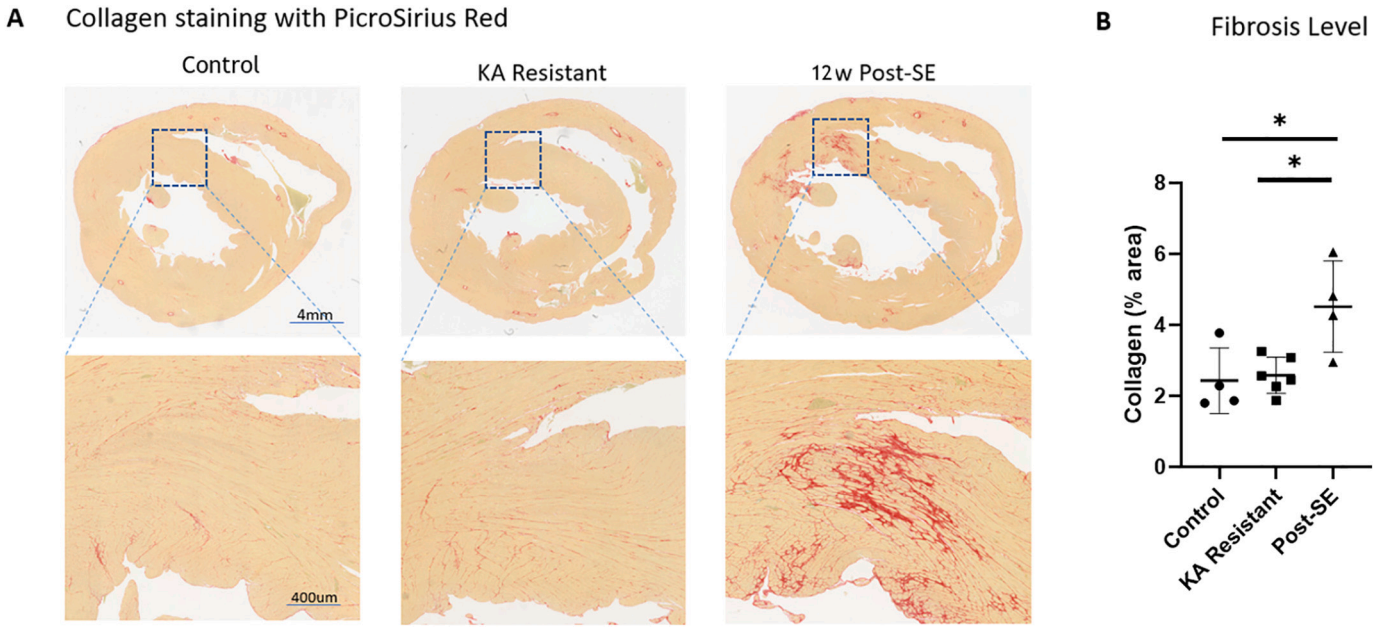

Fig. 6. Cardiac fibrosis is not related to systemic kainic acid injection. (A) Transverse sections of hearts showing collagen staining with picrosirius red in control, KA resistant and post-SE rats. (B) The collagen level (% area) in the post-SE ($n = 4$) was significantly higher compared to KA resistant ($n = 6$) to vehicle treated control (n = 4) groups. Statistical analysis was performed using one-way ANOVA, * $p < 0.05$. (For interpretation of the references to colour in this figure legend, the reader is referred to the web version of this article.)

despite an increased awareness of SUDEP over the last decade the diagnosis is still commonly overlooked by medical examiners, with the deaths attributed to cardiac disease, particularly when cardiac pathology is found on post-mortem in a patient with epilepsy (Panelli and O'Brien, 2019; Devinsky et al., 2017).

Therefore, this study serially studied cardiac function and structure in vivo, from before the development of epilepsy, through the epileptogenic period, and into the chronic epileptic state. The results demonstrate that chronic epilepsy in this rat model of TLE results in progressive long-term alterations in cardiac structure and function, consistent with a restrictive cardiomyopathy with myocardial fibrosis. The cardiac changes strongly resemble that seen in patients with chronic TLE, with a direct relationship between seizure frequency and the severity of the functional and structural cardiac changes. Our findings

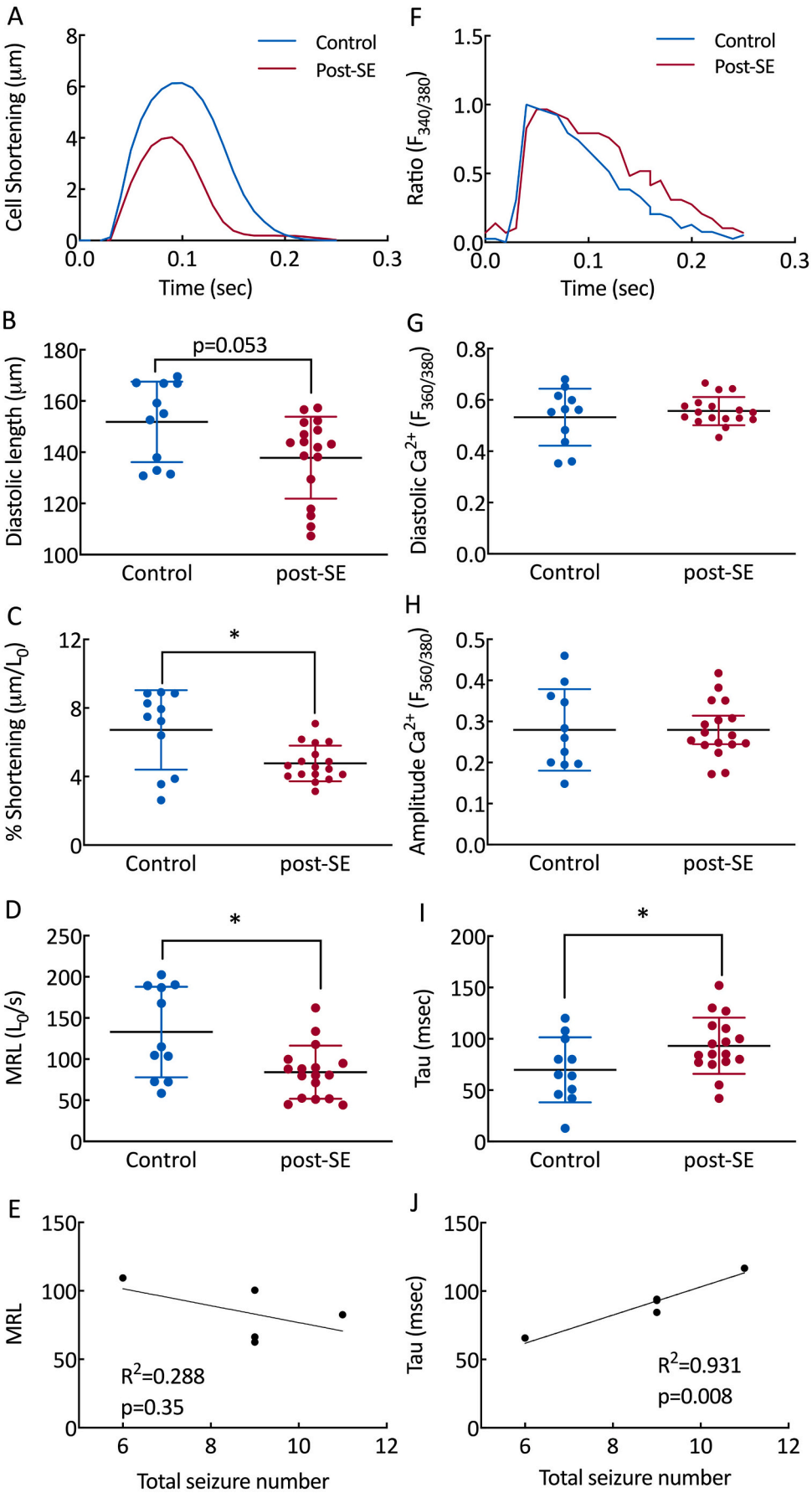

Fig. 5. Slowed cardiomyocyte relaxation and re-uptake of Ca^{2+} into the sarcoplasmic reticulum in post SE rats. (A and F) Fura-2 loaded isolated myocyte exemplar records: shortening and Ca^{2+} transients. Diastolic length (B) was shorter, % shortening (C) was reduced and maximum rate of lengthening (MRL) was slower in chronically epileptic rats. No significant correlation between MRL and seizure frequency was apparent (E). Cardiomyocyte diastolic (G) and amplitude (H) Ca^{2+} transient was not significantly different between groups, however the time to relaxation of the Ca^{2+} transient (tau) was significantly slowed in cardiomyocytes from epileptic hearts (I). A significant correlation between tau and seizure frequency was also apparent (J). Two-tailed Mann Whitney *U* test comparing saline and post-SE. *$p < 0.05$; $n = 11$–17 cells from $n = 3$–7 hearts/group.

Table 3
Cardiomyocyte calcium and contractility data.

Calcium Parameter	Control	Post-SE
Diastolic Ca^{2+} (ratio)	0.53 ± 0.03 (11)	0.56.1 ± 0.01 (17)
Systolic Ca^{2+} (ratio)	0.81 ± 0.05 (11)	0.84 ± 0.02 (17)
Amplitude Ca^{2+} (ratio)	0.28 ± 0.03 (11)	0.28 ± 0.07 (17)
Tau (msec)	69.91 ± 6.25 (11)	93.24 ± 6.64 (17)$^{\delta}$
Contractility Parameters		
Diastolic Length (μm)	151.9 ± 4.74 (11)	137.9 ± 3.87 (17)*
% Shortening	6.73 ± 0.70 (11)	4.77 ± 0.25 (17)$^{\delta\delta}$
Time to peak shortening (msec)	83.55 ± 4.05 (11)	83.29 ± 5.93 (17)
Max Rate of Shortening (L_0/s)	161.50 ± 16.59 (11)	115.87 ± 8.26 (17)$^{\delta}$
Max Rate of Lengthening (L_0/s)	133.10 ± 16.60 (11)	84.27 ± 7.81 (17)$^{\delta\delta}$
Time to Cycle Completion (msec)	174.00 ± 6.52 (11)	166.00 ± 8.94 (17)

* $p = 0.052$ Two-tailed Mann Whitney U test, $^{\delta}p < 0.05$, $^{\delta\delta}p < 0.01$, unpaired *t*-test; n = 11–17 cells, n = 3–7 hearts/group.

are broadly consistent with those of a previous study that examined EEGs, echocardiograms and post-mortem histology in separate groups of rats at 3 months and at 7–11 months post-KA SE in rats (Naggar et al., 2014), but unlike with our study myocardial fibrosis was not found. While our study did not have as long-term follow-up as the previous study, we performed serial echocardiograms and ECGs at baseline, and 2- and 10-weeks post-KA SE, allowing the evolution of the changes, and their relationship to the onset and burden of seizures in the early chronic epilepsy period, that was unable to be done in the previous study and was the primary aim of the current study.

4.1. Cardiac morphology and systolic function are altered in chronically epileptic rats

The findings of this study show that both cardiac function and structure were progressively altered during the epileptogenic period and into the chronic epileptic state. The morphology of the left ventricle was altered, with reduced left ventricular dimensions and chamber volumes resulting in altered systolic properties, seen as a reduction in overall cardiac output and ejection fraction on echocardiocardiogram. The strongest risk factor for SUDEP is high seizure frequency (Shorvon and Tomson, 2011), and this was consistent with our echocardiography findings whereby post-SE rats with the highest seizure frequency having the lowest cardiac output and ejection fraction and the most marked fibrosis on post-mortem histology. This reduction in cardiac output was primarily due to a reduction in the volume of the left ventricle during the relaxation phase of the cardiac cycle, diastole, while systolic morphological parameters did not differ significantly from control rats. This indicates that the properties of diastole may be underlying the cardiac dysfunction seen in post-SE rats. In support of findings from our animal model, a previous study in patients with epilepsy identified cardiac functional changes, including a reduction in ejection fraction and increased LV filling pressure (Bilgi et al., 2013).

4.2. Diastolic dysfunction in chronically epileptic rats is evident before systolic functional changes

Diastolic dysfunction also developed during epileptogenesis and with chronic epilepsy. The early phase of left ventricular filling showed normal blood flow into the left ventricle, but the time taken for this initial flow of blood was significantly reduced early in the epileptogenic period when spontaneous seizures are beginning to manifest. The deceleration time of the early filling phase is dependent on the ability of the ventricles to relax. This reduction in deceleration time indicates impediment that post-SE rats have non-compliant "stiff" LV walls ultimately leading to inadequate ventricle filling and reduced cardiac output. The E/E` ratio was also significantly increased 2 weeks post-SE and was still elevated in chronically epileptic rats 10 weeks post-SE. This ratio is the most important non-invasive indicator of LV filling pressure and reflects reduced compliance of the LV. Increased ventricular stiffness and higher filling pressures have been reported in patients with epilepsy (Fialho et al., 2018a; Bilgi et al., 2013) and in the same post-SE animal model used in this study (Naggar et al., 2014), providing valuable data supporting our findings.

A novel result from this study was the demonstration of the emergence of diastolic dysfunction at two weeks post-SE in the epileptic hearts before systolic dysfunction became apparent at 10 weeks. This indicates that the cardiac pathology associated with epilepsy is driven initially by a diastolic phenotype with increased stiffness in the ventricular wall preceding systolic dysfunction. Increased cardiac fibrosis, as shown histologically in the chronically epileptic rats in this study, is known to be one of the main contributors to increased cardiac stiffness and diastolic dysfunction (van Heerebeek et al., 2006; van Heerebeek et al., 2008).

4.3. Cardiac fibrosis plays a key role in cardiac dysfunction in chronically epileptic rats

Cardiac fibrosis, characterized by excessive deposition of extracellular matrix proteins, is a significant global health problem associated with nearly all forms of heart disease (van Heerebeek et al., 2006; van Heerebeek et al., 2008). Cardiac fibroblasts are an essential cell type in the heart whose role is to maintain homeostasis of the extracellular matrix (Travers et al., 2016). However, an imbalance of these processes results in fibroblast proliferation and fibrosis. Increased fibrosis ultimately results in wall stiffening, reduced contractility and impaired overall heart performance and promotes systolic and diastolic dysfunction and arrhythmogenesis (Travers et al., 2016). The effect of cardiac fibrosis on heart function and its link to increasing the risk of lethal arrhythmias in epilepsy has been highlighted in several studies (Nascimento et al., 2017; Fialho et al., 2018b; P-Codrea Tigaran et al., 2005). In chronically epileptic rats, we demonstrated significant left ventricular fibrosis, which is positively correlated to seizure frequency, highlighting the detrimental effect of repeated seizures on the heart. This also argues against the possibility that the systemic KA used to induce SE has a significant direct cardiotoxic effect that confounded the analysis of the relationship between the epilepsy and the functional and structural cardiac changes. Further supporting this is that cardiac fibrosis was not evident in the 6 KA resistant rats who received comparable doses of KA but did not go into SE or become chronically epileptic, but was again seen in the 4 rats in this cohort who did go into SE and then subsequently were confirmed to be epileptic on continuous EEG recordings at 12 weeks post-SE.

4.4. Slowed cardiomyocyte relaxation and re-uptake of Ca^{2+} into the sarcoplasmic reticulum contribute to diastolic dysfunction in chronically epileptic rats

In addition to cardiac fibrosis, intrinsic cardiomyocyte stiffness can also play a role in diastolic dysfunction (van Heerebeek et al., 2006; van Heerebeek et al., 2008). Slowed cardiomyocyte relaxation along with slowed Ca^{2+} uptake into the sarcoplasmic reticulum were both prevalent in the chronically epileptic rats. Whilst intrinsic cardiomyocyte stiffness was not measured in this study, the changes in these two parameters indicate alterations in diastolic properties of the cardiomyocyte which could be contributing to overall diastolic dysfunction in epileptic hearts. Interestingly, the slowed rate of cardiomyocyte lengthening was not significantly correlated with seizure frequency, however, the slowed uptake of Ca^{2+} into the SR was strongly correlated to seizure frequency. This indicates that the movement of Ca^{2+} ions within the cardiomyocyte to allow relaxation to occur is strongly dependent on the number of seizures present and implies that this process is linked to changes in cellular function with epilepsy. This reduction in Ca^{2+} uptake to the SR is usually associated with a dysregulation of the SR Ca^{2+} ATPase pump (SERCA2a) or changes to the phospholamban (PLB) protein (Sipido and

Vangheluwe, 2010; Sulaiman et al., 2010). Future investigation could include measurement of SERCA2a and PLB proteins and intact cardiomyocyte stiffness measurements.

4.5. Alteration in HRV measures suggesting cardiac autonomic dysfunction in chronically epileptic rats

The mechanisms for the functional and structure cardiac changes demonstrated here in the chronic epilepsy stage in the post-KA SE model of TLE remain to be elucidated, but the changes resemble those seen in chronic autonomic dysfunction with increased sympathetic tone (Gyongyosi et al., 2017; Ancona et al., 2016). A number of studies have demonstrated that patients and animals with chronic epilepsy have altered sympathetic tone (Fialho et al., 2018b; Naggar et al., 2014; Bhandare et al., 2017; Persson et al., 2005; Liu et al., 2018). The repeated cardiovascular "sympathetic storms" occurring from recurrent seizures over time in patients with drug-resistant chronic epilepsy may play a causative role in the cardiac dysfunction and fibrosis that we identified in the chronically epileptic rats in this study. To investigate this hypothesis further we undertook an analysis of HRV from the ECG recordings acquired during the continuous 2 weeks of video-EEG recording 11–13 weeks post-KA SE. Analysis of HRV is a widely used measure of neural cardiac control (Malliani et al., 1991). These demonstrated significantly lower RMSSD and significantly higher normalized LFP of the HRV in wakefulness compared to non-epileptic control rats (Table 4). The low RMSSM during wakefulness, indicative of lower HRV in the epileptic rats, is consistent with findings in human epilepsy cohorts where it has been found to be associated with drug-resistance and epilepsy chronicity (Myers et al., 2018), and predicts less favorable outcomes after epilepsy surgery and vagal nerve stimulator implantation (Persson et al., 2005; Liu et al., 2018). In non-epilepsy cohorts, low HRV has been shown to predict an increased risk of sudden death in heart disease patients (Kleiger et al., 1987; La Rovere et al., 1998; Galinier et al., 2000), and all-cause mortality in older adults (Tsuji et al., 1994). RMSSD is sensitive to rapid changes in heart rate mediated by the myelinated vagal efferents, it can be interpreted to reflect a decrease in parasympathetic drive to the heart. Conversely, LRF was increased. If one accepts that this indirect measure may reflect an increase in cardiac sympathetic drive, then these findings in the chronically epileptic rats post-KA SE evidence there could be a sympathetically-mediated mechanism that leads to the functional and, ultimately, the structural cardiac changes. In other words, the withdrawal of the cardioprotective parasympathetic outflow, coupled with an increase in proarythmogenic sympathetic drive to the heart, may establish functional changes that precipitate the structural changes reported herein. Indeed, we know that chronic stress leads to an increase in cardiac sympathetic drive that lead to cardiac dysrhythmias (Fontes et al., 2017) and major functional changes in the heart, as seen in Takotsubo syndrome (Devinsky et al., 2017). That these changes were only apparent in the awake state (there were no inter-goup differences in sleep) fits with what we know about autonomic control of the heart: during non-REM sleep there is a progressive increase in parasympathetic outflow and decrease in sympathetic outflow, as manifested by a reduction in heart rate, stroke volume, peripheral vascular resistance, blood pressure and respiration (Somers et al., 1993).

Table 4
Heart rate variability (HRV) findings among controls and post-SE rats.

HRV Metric and State†	Control (n = 6^)	Post-SE (n = 9)	*p*-value*
Awake			
SDNN (ms)	12.60 (10.03–15.53)	9.52 (8.68–15.07)	0.388
RMSSD (ms)	10.72 (9.32–17.24)	6.12 (3.88–10.25)	**0.036***
Normalized LFP (nu)	13.66 (10.70–15.30)	28.41 (18.21–41.58)	**0.012***
Normalized HFP (nu)	66.11 (60.05–71.97)	55.98 (48.34–68.74)	0.224
Sleep			
SDNN (ms)	12.87 (4.07–19.23)	10.80 (5.28–14.32)	0.607
RMSSD (ms)	11.48 (3.71–17.67)	6.06 (3.77–10.70)	0.607
Normalized LFP (nu)	8.38 (6.11–25.24)	21.00 (10.18–30.42)	0.224
Normalized HFP (nu)	65.29 (56.55–73.83)	63.40 (54.72–69.06)	0.607

†Values represent the median and IQR. HRV measures in each state (sleep or wakefulness) were assessed between groups by using a two-tailed Mann Whitney U test; ^In two control rats, suitable ECG data were not available. *Indicates a statistically significant finding; The standard deviation of the normal-to-normal intervals (SDNN); The root mean square of the successive differences (RMSSD); low-frequency power (LFP); high-frequency power (HFP).

Table 5
Correlation coefficient for HRV metrics and seizure frequency in the post-SE rats.

HRV Metric and State	Correlation Coefficient†	*p*-value
Sleep		
SDNN (ms)	0.778	0.018*
RMSSD (ms)	0.703	0.041*
Normalized LFP (nu)	0.251	0.511
Normalized HFP (nu)	0.075	0.853
Awake		
SDNN (ms)	0.343	0.363
RMSSD (ms)	0.611	0.088
Normalized LFP (nu)	0.008	0.991
Normalized HFP (nu)	0.025	0.957

†Correlation was calculated using the Spearman rank correlation coefficient. *Indicates statistical significance.

5. Conclusion

The results of this study demonstrate in the post-SE rat model of chronic TLE, that progressive changes in cardiac function, with decreased ejection fraction and diastolic dysfunction, and underlying cardiac fibrosis develop progressively with the development of chronic epilepsy. This is suggestive of a restrictive cardiomyopathy phenotype, and consistent with reports that have examined for this in patients with chronic epilepsy, including those who have died from SUDEP (Nascimento et al., 2017; Ramadan et al., 2013; Fialho et al., 2018b; Bilgi et al., 2013). The severity of the cardiac changes correlate with the seizure frequency, further supporting a direct effect of the chronic seizure burden. Cardiac fibrosis has been shown to be a risk factor for fatal arrhythmias and SUDEP (Fialho et al., 2018a; Gyongyosi et al., 2017), and may predispose sufferers to having arrhythmias and increased risk of SUDEP. While the mechanisms underlying these cardiac abnormalities in the chronically epileptic rats remains to be determined, we found evidence for abnormal cardiac autonomic function on analysis of HRV on the ECGs during wakefulness in the chronically epileptic rats.

Ethical statement

We confirm that we have read the Journal's position on issues involved in ethical publication and affirm that this report is consistent with those guidelines.

Funding

NHMRC project grant APP1082215 to KLP, LMD and TJO, NHMRC Program APP1091593 and Investigator APP1176426 Grants to TJO, and a start-up grant by Monash University to TJO. SS is supported by a Bridging Postdoctoral Fellowship from Monash University (BPF20-3253672466) and the Victorian Medical Research Acceleration Fund. VGM is supported by a Baker Fellowship. PMCE was funded by an NHMRC Early Career Fellowship (#APP1087172).

Declaration of Competing Interest

None of the authors has any conflict of interest to disclose.

Appendix A. Supplementary data

Supplementary data to this article can be found online at https://doi.org/10.1016/j.nbd.2021.105505.

References

Ancona, F., Bertoldi, L.F., Ruggieri, F., et al., 2016 Oct 1. Takotsubo cardiomyopathy and neurogenic stunned myocardium: similar albeit different. Eur. Heart J. 37 (37), 2830–2832.

Bhandare, A.M., Kapoor, K., Powell, K.L., et al., 2017 May 14. Inhibition of microglial activation with minocycline at the Intrathecal level attenuates Sympathoexcitatory and Proarrhythmogenic changes in rats with chronic temporal lobe epilepsy. Neuroscience. 350, 23–38.

Bilgi, M., Yerdelen, D., Colkesen, Y., Muderrisoglu, H., 2013 Sep. Evaluation of left ventricular diastolic function by tissue Doppler imaging in patients with newly diagnosed and untreated primary generalized epilepsy. Seizure. 22 (7), 537–541.

Casillas-Espinosa, P.M., Shultz, S.R., Braine, E.L., et al., 2019 Nov. Disease-modifying effects of a novel T-type calcium channel antagonist, Z944, in a model of temporal lobe epilepsy. Prog. Neurobiol. 182, 101677.

Chyou, J.Y., Friedman, D., Cerrone, M., et al., 2016 Jul. Electrocardiographic features of sudden unexpected death in epilepsy. Epilepsia. 57 (7), e135–e139.

Curl, C.L., Danes, V.R., Bell, J.R., et al., 2018 Jun. Cardiomyocyte functional etiology in heart failure with preserved ejection fraction is distinctive-A new preclinical model. J. Am. Heart Assoc. 1, 7(11).

Devinsky, O., Friedman, D., Cheng, J.Y., Moffatt, E., Kim, A., Tseng, Z.H., 2017 Aug 29. Underestimation of sudden deaths among patients with seizures and epilepsy. Neurology. 89 (9), 886–892.

Fialho, G.L., Pagani, A.G., Wolf, P., Walz, R., Lin, K., 2018 Feb 2. Echocardiographic risk markers of sudden death in patients with temporal lobe epilepsy. Epilepsy Res. 140, 192–197.

Fialho, G.L., Wolf, P., Walz, R., Lin, K., 2018 Jun. Increased cardiac stiffness is associated with autonomic dysfunction in patients with temporal lobe epilepsy. Epilepsia. 59 (6), e85–e90.

Ficker, D.M., 2000. Sudden unexplained death and injury in epilepsy. Epilepsia. 41 (Suppl. 2), S7–12.

Ficker, D.M., So, E.L., Shen, W.K., et al., 1998 Nov. Population-based study of the incidence of sudden unexplained death in epilepsy. Neurology. 51 (5), 1270–1274.

Fontes, M.A.P., Limborco, M., Machado, N.L.S., et al., 2017 Nov. Asymmetric sympathetic output: the dorsomedial hypothalamus as a potential link between emotional stress and cardiac arrhythmias. Auton. Neurosci.-Basic. 207, 22–27.

Galinier, M., Pathak, A., Fourcade, J., et al., 2000 Mar. Depressed low frequency power of heart rate variability as an independent predictor of sudden death in chronic heart failure. Eur. Heart J. 21 (6), 475–482.

Gyongyosi, M., Winkler, J., Ramos, I., et al., 2017 Feb. Myocardial fibrosis: biomedical research from bench to bedside. Eur. J. Heart Fail. 19 (2), 177–191.

van Heerebeek, L., Borbely, A., Niessen, H.W., et al., 2006 Apr 25. Myocardial structure and function differ in systolic and diastolic heart failure. Circulation. 113 (16), 1966–1973.

van Heerebeek, L., Hamdani, N., Handoko, M.L., et al., 2008 Jan 1. Diastolic stiffness of the failing diabetic heart: importance of fibrosis, advanced glycation end products, and myocyte resting tension. Circulation. 117 (1), 43–51.

Hellier, J.L., Patrylo, P.R., Buckmaster, P.S., Dudek, F.E., 1998 Jun. Recurrent spontaneous motor seizures after repeated low-dose systemic treatment with kainate: assessment of a rat model of temporal lobe epilepsy. Epilepsy Res. 31 (1), 73–84.

Jehi, L., Najm, I.M., 2008 Mar. Sudden unexpected death in epilepsy: impact, mechanisms, and prevention. Cleve. Clin. J. Med. 75 (Suppl. 2), S66–S70.

Jupp, B., Williams, J., Binns, D., et al., 2012 Jul. Hypometabolism precedes limbic atrophy and spontaneous recurrent seizures in a rat model of TLE. Epilepsia. 53 (7), 1233–1244.

Kleiger, R.E., Miller, J.P., Bigger, J.T., Moss, A.J., 1987 Feb 1. Decreased heart-rate-variability and its association with increased mortality after acute myocardial-infarction. Am. J. Cardiol. 59 (4), 256–262.

Kwan, P., Schachter, S.C., Brodie, M.J., 2011 Sep 8. Drug-resistant epilepsy. N. Engl. J. Med. 365 (10), 919–926.

La Rovere, M.T., Bigger, J.T., Marcus, F.I., Mortara, A., Schwartz, P.J., Investigators, A., 1998 Feb 14. Baroreflex sensitivity and heart-rate variability in prediction of total cardiac mortality after myocardial infarction. Lancet. 351 (9101), 478–484.

Liu, H.Y., Yang, Z., Meng, F.G., et al., 2018 Mar. Preoperative heart rate variability as predictors of vagus nerve stimulation outcome in patients with drug-resistant epilepsy. Sci. Rep.-UK. 1, 8.

Malik, M., 1996 Mar 1. Heart rate variability: standards of measurement, physiological interpretation and clinical use. Task force of the European Society of Cardiology and the north American Society of Pacing and Electrophysiology. Circulation. 93 (5), 1043–1065.

Malliani, A., Pagani, M., Lombardi, F., Cerutti, S., 1991 Aug. Cardiovascular neural regulation explored in the frequency-domain. Circulation. 84 (2), 482–492.

Myers, K.A., Sivathamboo, S., Perucca, P., 2018 Dec. Heart rate variability measurement in epilepsy: how can we move from research to clinical practice? Epilepsia. 59 (12), 2169–2178.

Naggar, I., Lazar, J., Kamran, H., Orman, R., Stewart, M., 2014 Jan. Relation of autonomic and cardiac abnormalities to ventricular fibrillation in a rat model of epilepsy. Epilepsy Res. 108 (1), 44–56.

Nascimento, F.A., Tseng, Z.H., Palmiere, C., et al., 2017 Aug. Pulmonary and cardiac pathology in sudden unexpected death in epilepsy (SUDEP). Epilepsy Behav. 73, 119–125.

Nightscales, R., McCartney, L., Auvrez, C., et al., 2020 Aug 11. Mortality in patients with psychogenic nonepileptic seizures. Neurology. 95 (6) e643-e52.

Panelli, R.J., O'Brien, T.J., 2019 Sep. Epilepsy and seizure-related deaths: mortality statistics do not tell the complete story. Epilepsy Behav. 98 (Pt A), 266–272.

P-Codrea Tigaran, S., Dalager-Pedersen, S., Baandrup, U., Dam, M., Vesterby-Charles, A., 2005 Jun. Sudden unexpected death in epilepsy: is death by seizures a cardiac disease? Am J Forensic Med Pathol 26 (2), 99–105.

Persson, H., Kumlien, E., Ericson, M., Tomson, T., 2005 Oct 11. Preoperative heart rate variability in relation to surgery outcome in refractory epilepsy. Neurology. 65 (7), 1021–1025.

Powell, K.L., Ng, C., O'Brien, T.J., et al., 2008 Oct. Decreases in HCN mRNA expression in the hippocampus after kindling and status epilepticus in adult rats. Epilepsia. 49 (10), 1686–1695.

Powell, K.L., Jones, N.C., Kennard, J.T., et al., 2014 Apr. HCN channelopathy and cardiac electrophysiologic dysfunction in genetic and acquired rat epilepsy models. Epilepsia. 55 (4), 609–620.

Ramadan, M., El-Shahat, N., Omar, A., et al., 2013. Interictal electrocardiographic and echocardiographic changes in patients with generalized tonic-clonic seizures. Int. Heart J. 54 (3), 171–175.

Read, M.I., McCann, D.M., Millen, R.N., Harrison, J.C., Kerr, D.S., Sammut, I.A., 2015 Nov. Progressive development of cardiomyopathy following altered autonomic activity in status epilepticus. Am. J. Physiol. Heart Circ. Physiol. 309 (9), H1554–H1564.

Sharma, S., Mazumder, A.G., Rana, A.K., Patial, V., Singh, D., 2019 Aug. Spontaneous recurrent seizures mediated cardiac dysfunction via mTOR pathway upregulation: a putative target for SUDEP management. CNS Neurol. Disord. Drug Targets 1.

Shorvon, S., Tomson, T., 2011 Dec 10. Sudden unexpected death in epilepsy. Lancet. 378 (9808), 2028–2038.

Sipido, K.R., Vangheluwe, P., 2010 Feb 5. Targeting sarcoplasmic reticulum Ca2+ uptake to improve heart failure: hit or miss. Circ. Res. 106 (2), 230–233.

Somers, V.K., Dyken, M.E., Mark, A.L., Abboud, F.M., 1993 Feb 4. Sympathetic-nerve activity during sleep in normal subjects. N. Engl. J. Med. 328 (5), 303–307.

Sulaiman, M., Matta, M.J., Sunderesan, N.R., Gupta, M.P., Periasamy, M., Gupta, M., 2010 Mar. Resveratrol, an activator of SIRT1, upregulates sarcoplasmic calcium ATPase and improves cardiac function in diabetic cardiomyopathy. Am. J. Physiol. Heart Circ. Physiol. 298 (3), H833–H843.

Surges, R., Taggart, P., Sander, J.W., Walker, M.C., 2010 May. Too long or too short? New insights into abnormal cardiac repolarization in people with chronic epilepsy and its potential role in sudden unexpected death. Epilepsia. 51 (5), 738–744.

Travers, J.G., Kamal, F.A., Robbins, J., Yutzey, K.E., Blaxall, B.C., 2016 Mar 18. Cardiac fibrosis: the fibroblast awakens. Circ. Res. 118 (6), 1021–1040.

Tsuji, H., Venditti, F.J., Manders, E.S., et al., 1994 Aug. Reduced heart-rate-variability and mortality risk in an elderly cohort - the Framingham heart-study. Circulation. 90 (2), 878–883.